Climate Dynamics (2022) 59:1981–1996
https://doi.org/10.1007/s00382-022-06192-6

Interdecadal change in the relationship between El Niño in the decaying stage and the central China summer precipitation

Lin Chen[1] · Gen Li[1,2]

Received: 24 October 2021 / Accepted: 2 February 2022 / Published online: 23 March 2022

Abstract

Year-to-year variations of summer precipitation over the densely populated central China can exert great impacts on the local society and economy. Using the observed and reanalyzed datasets for the period 1960–2020, this study investigates the relationship between the decaying El Niño and the central China summer precipitation (CCSP). The results show that the central China tends to feature excessive precipitation during post-El Niño summers. In particular, we find that such a climatic effect of El Niño exhibits an evident interdecadal strengthening since the early 1990s. This is due to the changing intensity and duration of the El Niño events. Compared to the prior decades (1960–1992), there are stronger intensity and longer duration of the El Niño-related warm sea surface temperature (SST) anomalies in the tropical central Pacific in the epoch after the early 1990s (1993–2020). Through the Walker circulation adjustment, the strengthened intensity and longer duration of the central Pacific SST anomalies cause stronger and longer-lasting easterly anomalies along the equatorial Indian Ocean, which can further intensify the SST warming over the Southwest Indian Ocean (SWIO) in boreal spring following El Niño by forcing a downwelling Rossby wave. The robust SWIO warming induces stronger Indian Ocean basin-wide SST warming and anomalous anticyclone over the Northwest Pacific in post-El Niño summers through initiating a series of ocean-atmospheric interactions. As a result, the anomalous anticyclone would deliver the abundant water vapor to the central China and contribute to increased local summer precipitation. By contrast, in the prior epoch (1960–1992), the El Niño-related SST warming in the central Pacific is relatively weaker and shorter-lasting, which results in weaker Indo-Pacific climate interactions in the decaying summer, thus having no significant impact on the CCSP. Our results highlight a strengthening influence of El Niño on the following summer precipitation over the central China since the early 1990s. This has important implications for the regional seasonal climate prediction.

Keywords Interdecadal change · El Niño · Central China summer precipitation · Decaying stage · East Asian summer monsoon · Atmospheric teleconnection

1 Introduction

The densely populated central China is penetrated by the two largest rivers of China, the Yangtze River and the Yellow River, and is an important agricultural and industrial area in China (Sun et al. 2010; Ren et al. 2013; Ke and Guan 2014; Hu et al. 2020; Chen et al. 2021). Summer floods, landslides and mudslides brought by the heavy precipitation are the major disasters in this region, which often cause enormous damages to the local society and economy (Gao et al. 2020a, b; Hu et al. 2020). For example, the long-persisting Meiyu season over the Yangtze River basin in the summer of 2020 (Liu et al. 2020; Zhou et al. 2021; Ding et al. 2021; Qiao et al. 2021; Wang et al. 2021; Zheng and Wang 2021) and the torrential precipitation over the Henan Province in July of 2021 seriously destroyed the basic living conditions of human beings and caused enormous economic losses. Therefore, it is of great importance to investigate the nature and causes of the interannual variability of the central China summer precipitation (CCSP).

El Niño, as an important source of interannual climate variability worldwide, can significantly affect the summer climate over the East Asia (including the central China) in its

✉ Gen Li
ligen@hhu.edu.cn

[1] College of Oceanography, Hohai University, Nanjing, China

[2] Southern Marine Science and Engineering Guangdong Laboratory (Zhuhai), Zhuhai, China

decaying stage via the atmospheric teleconnection (Zhang et al. 1999, 2017; Wang et al. 2000; Chen 2002; Wu et al. 2009, 2010; Xie et al. 2009, 2016; Jin et al. 2016; Hu et al. 2017, 2019, 2020; He et al. 2019; Jiang et al. 2019; Sun et al. 2021). In post-El Niño summers, the central China often exhibits significant positive precipitation anomalies (Wu et al. 2009; Xie et al. 2009; Hu et al. 2017, 2020). Previous studies suggested that such excessive precipitation anomalies over the central China are closely associated with the El Niño-induced atmospheric circulations (Wu et al. 2009; Xie et al. 2009; Hu et al. 2017, 2020) and the local topography (Hu et al. 2017, 2020). Usually, there is an anomalous anticyclone over the Northwest Pacific (NWP) in post-El Niño summers, which could strengthen the East Asian summer monsoon and deliver the abundant warm-humid flow to the north (Chang et al. 2000a, b; Wang et al. 2000, 2013; Xie et al. 2009; Li et al. 2017, 2021a; Tao et al. 2017, 2018; Jiang et al. 2019; Hu et al. 2017, 2019, 2020; He et al. 2019; Tang et al. 2021). As the central China contains numerous mountain ranges including the Wushan, Bashan, Qinling and Tai-hang mountains from the southwest to the northeast, when the warm-humid flow arrives at the mountains, local precipitation increases through the orographic lift (Hu et al. 2017, 2020). Apparently, the anomalous Northwest Pacific anticyclone (NWPAC) plays a crucial role in bridging the El Niño events and the CCSP. Thus, a better understanding of the effect of the preceding winter El Niño on the following summer NWPAC is vitally important for the seasonal prediction of the CCSP.

The Indian Ocean basin-wide sea surface temperature (SST) warming induced by El Niño is essential for the El Niño-NWPAC teleconnection (Yang et al. 2007; Xie et al. 2009; Chen et al. 2016, 2019; Li et al. 2017; Jiang et al. 2019; Wang 2019; Sun et al. 2021; Wu et al. 2021). It acts like a capacitor, which starts charging in the El Niño developing autumn and maturing winter and discharging in the decaying summer, explaining why the El Niño-related atmospheric circulation anomalies can still exist in the following summer despite that the tropical central and eastern Pacific SST anomalies have largely dissipated (Yang et al. 2007; Xie et al. 2009; Cai et al. 2019). Specifically, in response to the anomalous SST warming in the tropical central and eastern Pacific, anomalous easterly winds appear over the equatorial Indian Ocean in the El Niño developing autumn and mature winter through the Walker circulation adjustment (Alexander et al. 2002; Lau and Nath 2003; Du et al. 2009). They support anomalous anticyclonic wind curls over the Southeast Indian Ocean (SEIO) and force the downwelling Rossby waves that slowly propagate to the west Masumoto and Meyers (1998; Yu et al. 2005; Du et al. 2009; Xie et al. 2010; Cai et al. 2019; Wang 2019). When the westward-propagating downwelling Rossby waves arrive at the Southwest Indian Ocean (SWIO) during the El Niño decaying spring where the mean thermocline is shallow and the thermocline feedback is strong (Du et al. 2009; Chen et al. 2019), the local SST would significantly warm. Subsequently, the SWIO warming intensifies the atmospheric convection and triggers an antisymmetric wind pattern with the northeasterlies in the north and the northwestlies in the south of the equator (Wu et al. 2008; Du et al. 2009; Wu and Yeh 2010; Cai et al. 2019; Chen et al. 2019; Chowdary et al. 2019). This antisymmetric wind pattern would persist until boreal summer and weaken the Indian Ocean monsoon, contributing to the basin-wide SST warming through the wind-evaporation-SST feedback (Du et al. 2009; Xie et al. 2010; Cai et al. 2019; Chen et al. 2019). Such a basin-wide SST warming in post-El Niño summers excites a warm Kelvin wave penetrating into the NWP, thus inducing the anomalous NWPAC (Yang et al. 2007; Xie et al. 2009; Chowdary et al. 2010; Jiang et al. 2013; Li et al. 2017, 2019; Zhou et al. 2018; Cai et al. 2019; Wang 2019; Sun et al. 2021).

Furthermore, there are strong coupled ocean-atmosphere interactions between the NWPAC and the SST anomalies in the Indo-Pacific region (Kosaka et al. 2013; Wang et al. 2013, 2020; Xie et al. 2016; Chowdary et al. 2019; Li et al. 2019; Jiang et al. 2019; Takaya et al. 2021). On the one hand, the anomalous northeasterly winds on the southeast flank of the NWPAC superimposing on the northeast trade winds would contribute to anomalous cooling in the NWP. The resultant NWP cooling would, in turn, induce the downwelling Rossby waves that enhance the NWPAC (Wang et al. 2013; Xie et al. 2016; Zhou et al. 2019). On the other hand, the anomalous easterlies on the south flank of the NWPAC can extent to the Indian Ocean, weakening the monsoonal winds and thus favoring the Indian Ocean warming (Kosaka et al. 2013). The resultant Indian Ocean warming would, in turn, help sustain the NWPAC through the warm Kelvin waves (Xie et al. 2016; Li et al. 2019; Zhou et al. 2019; Takaya et al. 2021). All this constitutes a positive feedback between the anomalous NWPAC and the Indian Ocean basin-wide SST warming. This is known as the Indo-western Pacific Ocean capacitor (IPOC) effect (Xie et al. 2016), illustrating the importance of the Indian Ocean basin-wide SST warming for the anomalous NWPAC in post-El Niño summers.

However, the IPOC effect may be sensitive to the intensity and decaying feature of the El Niño events (Xie et al. 2016; Wang et al. 2017a). We believe that stronger and sustained El Niño-related SST anomalies over the equatorial central and eastern Pacific may tend to excite more robust responses over the Indian Ocean and the NWP in the decaying summer. Since the early 1990s, the characters of the El Niño events are experiencing an obvious interdecadal

change, featuring an increasing intensity of the equatorial central Pacific SST anomalies (Yeh et al. 2009; Lee and McPhaden 2010; McPhaden et al. 2011). Recently, Li et al. (2021b) further demonstrate that the El Niño-related central Pacific SST anomalies also feature a longer duration since the early 1990s, with a robust warming still maintaining in the decaying spring. These mean that the El Niño-induced Indo-Pacific responses might be also strengthened. Here two questions are proposed: Is the relationship between the decaying El Niño and the CCSP strengthened since the early 1990s? If so, whether and how the strengthened relationship is modulated by the El Niño-induced Indian Ocean responses?

The present study investigates the decaying El Niño's effect on the CCSP. Indeed, we find that there is a strengthening influence of El Niño in the decaying stage on the CCSP since the early 1990s. Our results show that such an interdecadal change is associated with the stronger intensity and longer duration of the El Niño-related warm SST anomalies over the equatorial central Pacific, which could induce stronger climate responses over the Indo-Pacific Ocean in the decaying summer. As a result, a stronger anomalous NWPAC in post-El Niño summers could increase the CCSP by strengthening the summer monsoon. This implies that El Niño is becoming a more important predictor for the summer climate over the central China.

The rest of this paper is organized as follows. Section 2 describes the datasets and methods used in this study. Section 3 shows an interdecadal change in the effects of El Niño in the decaying stage on the CCSP. Section 4 analyzes the possible mechanisms for this interdecadal change. Section 5 is conclusions with discussions.

2 Datasets and methods

Multiple datasets for the period 1960–2020 are used in this study, including the monthly precipitation data from the University of East Anglia Climate Research Unit land-based gridded observations (CRU, TS4.02; 0.5°×0.5°; Harris et al. 2014), the monthly SST data taken from the Hadley Centre of the U.K. Met Office (HadISST; 1.0°×1.0°; Rayner et al. 2006), as well as the monthly atmospheric datasets derived from the National Centers for Environmental Prediction-National Center for Atmospheric Research (NCEP-NCAR) reanalysis (2.5°×2.5°; Kalnay et al. 1996). The monthly sea surface height (SSH) data, covering the period of 1958–2017, is also used in this study, which is taken from the European Centre for Medium-Range Weather Forecasts (ECMWF) Ocean Reanalysis System 4 (ORAS4; 1.0°×1.0°; Balmaseda et al. 2012).

To explore the relationship between the decaying El Niño and the CCSP, the CCSP index is denoted as the precipitation anomalies averaged over the region of 28°N-38°N, 100°E-118°E, and the Niño3.4 index, defined as the area-averaged (5°S-5°N, 170°W-120°W) SST anomalies, is used to track the El Niño events. Here, the 3-month running mean Niño3.4 index exceeding the threshold of 0.5 °C and persisting for 5 months is defined as an El Niño event. According to this criterion, we pick out 16 El Niño events during the prior and post epoch, which are listed in Table 1. To distinguish the phase of El Niño, we use 0 to represent the developing stage and 1 to mark the decaying stage. We denote the El Niño developing autumn [September-October-November (SON)] as SON(0), the mature winter [December-January-February (DJF)] is denoted as D(0)JF(1), and the following spring [March-April-May (MAM)] and summer [June-July-August (JJA)] are symbolized as MAM(1) and JJA(1), respectively. As we investigate the interdecadal change in the interannual relationship, all data are linearly detrended despite that the results are almost the same before and after removing the long-term trend. The statistical significance is tested via the two-tailed Student's *t* test.

3 Interdecadal change in the relationships between the decaying El Niño and the CCSP

The El Niño events can significantly affect the central China precipitation in the decaying summer through the atmospheric teleconnection (Xie et al. 2009; Wu et al. 2009; Hu et al. 2017, 2020). In Fig. 1a, we present the spatial distribution of the correlations between the preceding DJF Niño3.4 index and the following JJA precipitation over China during 1960–2020. Indeed, there are significant positive correlations dominating the region of the central China, with large values in the middle reaches of the Yangtze River basin and the Yellow River basin, indicating that the CCSP anomalies are closely associated with the preceding DJF SST anomalies in the equatorial central and eastern Pacific. The correlation coefficient between the preceding DJF Niño3.4 index and the CCSP index for the whole period is 0.34 with a significance level of $p < 0.01$ (Fig. 1b), further suggesting that there is an evident relationship between the decaying El Niño and the CCSP.

Table 1 A list of the El Niño events during 1960–1992 and 1993–2020

Period	Year
1960-1992	1963/1964, 1965/1966, 1969/1970, 1972/1973, 1977/1978, 1982/1983, 1987/1988, 1991/1992
1993–2020	1994/1995, 1997/1998, 2002/2003, 2004/2005, 2006/2007, 2009/2010, 2015/2016, 2018/2019

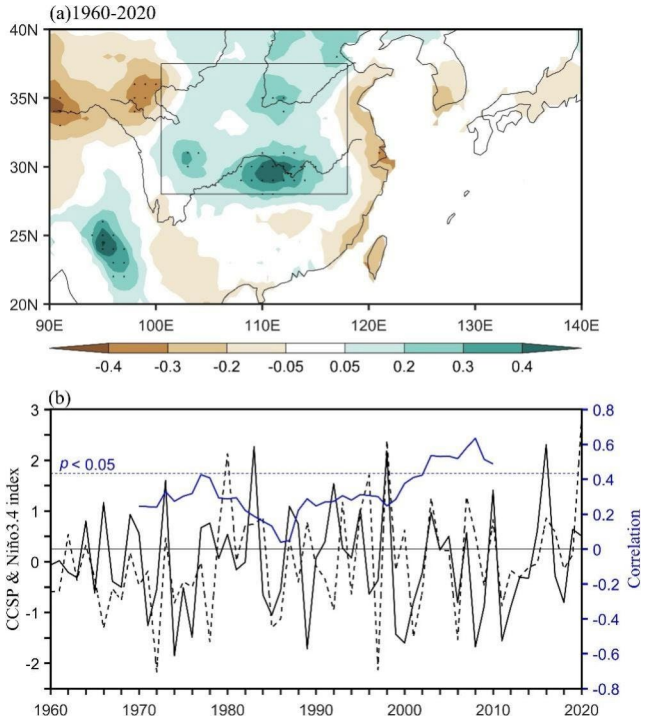

Fig. 1 **a** Correlation coefficients of the winter [December-January-February (DJF)] Niño3.4 (5°S-5°N, 170°W-120°W) index with the following summer [June-July-August (JJA)] precipitation anomalies during 1960–2020. The dots indicate that the correlations are at a significance level of $p < 0.05$. The box area denotes the region of the central China (28°N-38°N, 100°E-118°E). **b** Interannual time series of the DJF Niño3.4 index (solid black line) and the central China summer precipitation (CCSP) index (dashed black line) during 1960–2020. The solid blue line denotes the 21-year moving correlation coefficients between the two. The dashed blue line denotes the significance levels of $p < 0.05$. All data are linearly detrended and standardized

However, this interannual relationships between the decaying El Niño and the CCSP are unstable for the present study period. According to the 21-year moving correlations between the preceding DJF Niño3.4 index and the following JJA precipitation anomalies averaged in the central China, we identify that the correlation coefficients exhibit an evident change in the early 1990s. Specifically, the 21-year moving correlations in Fig. 1b are low and insignificant during 1960–1992 (the prior epoch), but dramatically strengthened during 1993–2020 (the post epoch). This means that there is a strengthened relationship between the decaying El Niño and the CCSP since the early 1990s, and the significant correlation between the decaying El Niño and the CCSP during the whole period is a result of this strengthened relationship.

To further show the difference in the relationship between the decaying El Niño and the JJA precipitation over the central China between the prior and post epochs, we compare the spatial distributions of the correlations between the JJA precipitation anomalies over China and the preceding DJF Niño3.4 index during these two epochs (Fig. 2). Remarkably, correlation coefficients in the most areas of the central China are inconspicuous during the prior epoch. While in the post epoch, significant positive correlations dominate the region of the central China, indicating a stronger influence of the decaying El Niño on the CCSP in this period (Fig. 2b). We also notice that the strong positive correlation coefficients go along the Wushan, Bashan, Qinling and Tai-hang mountains from the southwest to the northeast (Fig. 2b), indicating the role of the mountainous topography of the central China in anchoring the strengthened effect of El Niño since the early 1990s.

Such an interdecadal change between the El Niño events and the CCSP is also presented by the spatial distributions of the correlations between the preceding SON (and DJF) SST anomalies and the CCSP index during the prior and

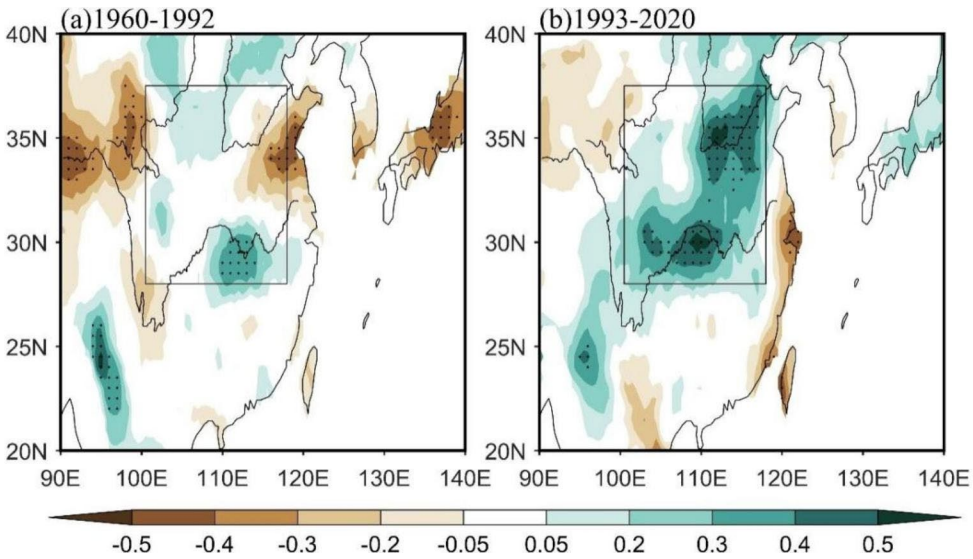

Fig. 2 Correlation coefficients of the DJF Niño3.4 index with the following summer precipitation anomalies during **a** 1960–1992 and **b** 1993–2020. The dots indicate that the correlations are at a significance level of $p < 0.05$. The box area in each panel denotes the region of the central China. All data are linearly detrended

post epochs (Fig. 3). In the prior epoch, the CCSP anomalies exhibit weak correlations with the tropical SST anomalies, and the significant correlations only exist in the tropical eastern Pacific (Fig. 3a, c). By contrast, in the post epoch, the correlations are much stronger and exhibit a significant El Niño-related SST anomaly pattern developing in SON and maturing in DJF, indicative of a strengthened relationship between the El Niño events and the CCSP anomalies since the early 1990s (Fig. 3b, d).

As the Indian Ocean responses are closely associated with the El Niño events, the SST anomaly pattern in the Indian Ocean also exhibits stronger correlations in the post epoch. Specifically, compared with almost no significant correlations in the Indian Ocean for the prior epoch (Fig. 3a, c), the correlations for the post epoch exhibit a prominent Indian Ocean dipole pattern in SON changing into an Indian Ocean basin mode in DJF with the development of the El Niño events (Fig. 3b, d). The SON cooling in the SEIO is a response to the strong upwelling off Java and Sumatra, which is forced locally by the stronger alongshore winds (Saji et al. 1999; Murtugudde et al. 2000). As El Niño matures in DJF, the enhanced solar radiation

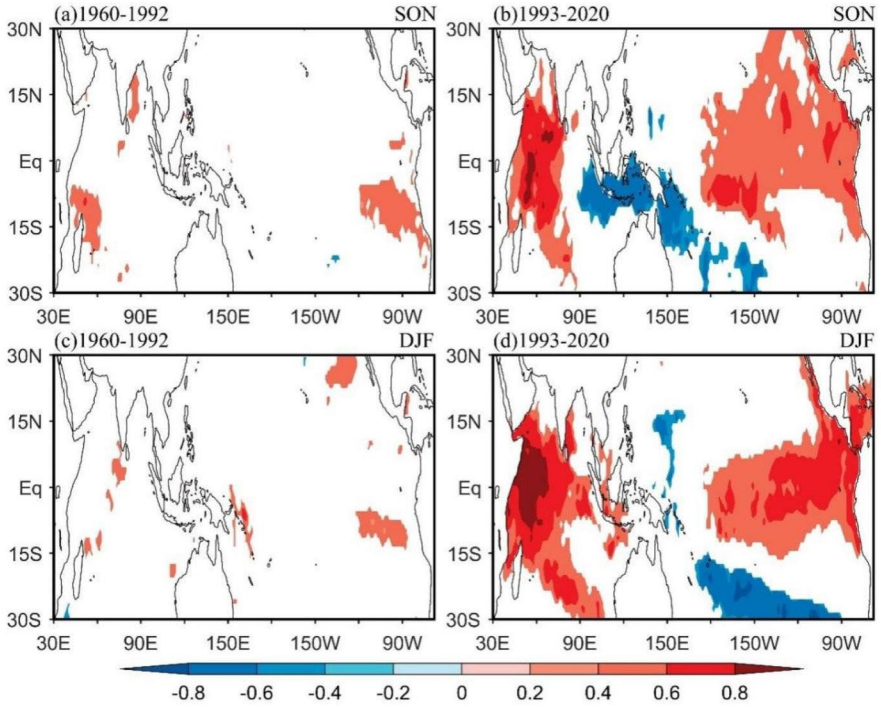

Fig. 3 Correlation coefficients of the CCSP index with **a** the preceding autumn [September-October-November (SON)] and **c** the preceding DJF sea surface temperature (SST) anomalies during 1960–1992. **b** and **d** Same as **a** and **c**, but for 1993–2020. The correlations are presented at a significance level of $p < 0.05$. All data are linearly detrended

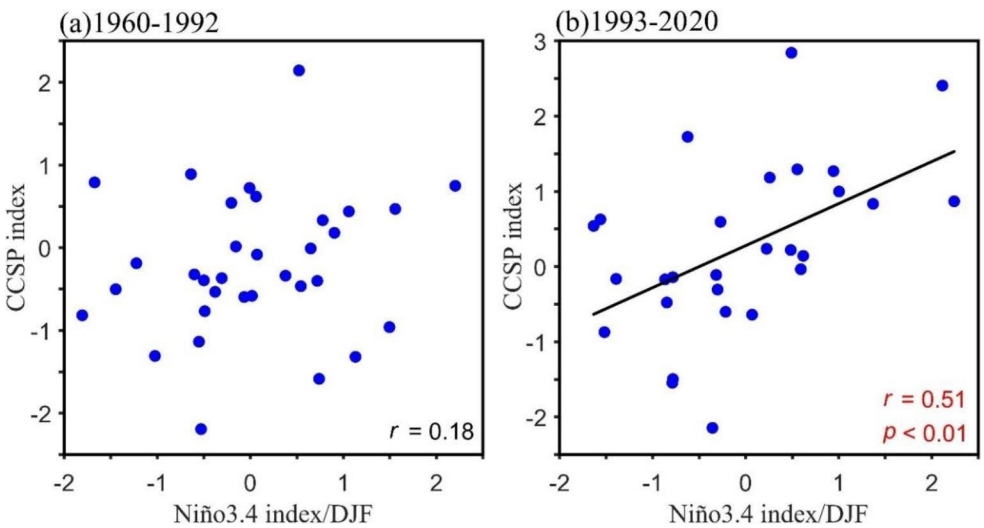

Fig. 4 Scatterplots of the CCSP index with the preceding DJF Niño3.4 index during **a**1960–1992 and **b** 1993–2020. Black line and *r* denote the linear fit and the correlation coefficient between the CCSP index and the Niño3.4 index, respectively. All data are linearly detrended and standardized

would contribute to a rapid warming in the SEIO, while the El Niño-induced downwelling Rossby waves in the SEIO would propagate to the west and contribute to anomalous warming in the SWIO. Therefore, there is a basin-wide SST warming in the Indian Ocean in the El Niño maturing winter (Shinoda et al. 2004; Chowdary and Gnanaseelan 2007; Du et al. 2009). The more significant charging process of the Indian Ocean with the development of El Niño in the post epoch further suggests that there might be a strengthened El Niño-CCSP relationship since the early 1990s.

Figure 4 shows the scatter plots between the preceding DJF Niño3.4 index and the following JJA precipitation anomalies averaged over the central China during the prior and post epochs, respectively. Obviously, the correlation coefficient in the prior epoch is low and insignificant (Fig. 4a). In contrast, in the post epoch, the correlation coefficient is 0.51 with a significance level of $p < 0.01$ (Fig. 4b). Furthermore, the correlation coefficients of the preceding DJF Niño3.4 index with the CCSP index during the negative ENSO phases in 1960–1992 and 1993–2020 are −0.06 and −0.17, respectively, which are both low and insignificant. All this further indicates that there is a strengthened El Niño-CCSP since the early 1990s and the La Niña-CCSP relationship is almost unchanged before and after the early 1990s.

4 Possible mechanisms for the strengthening influence of El Niño

4.1 Interdecadal change in El Niño

There is a close relationship between the decaying El Niño and the CCSP, with the central China often suffering a

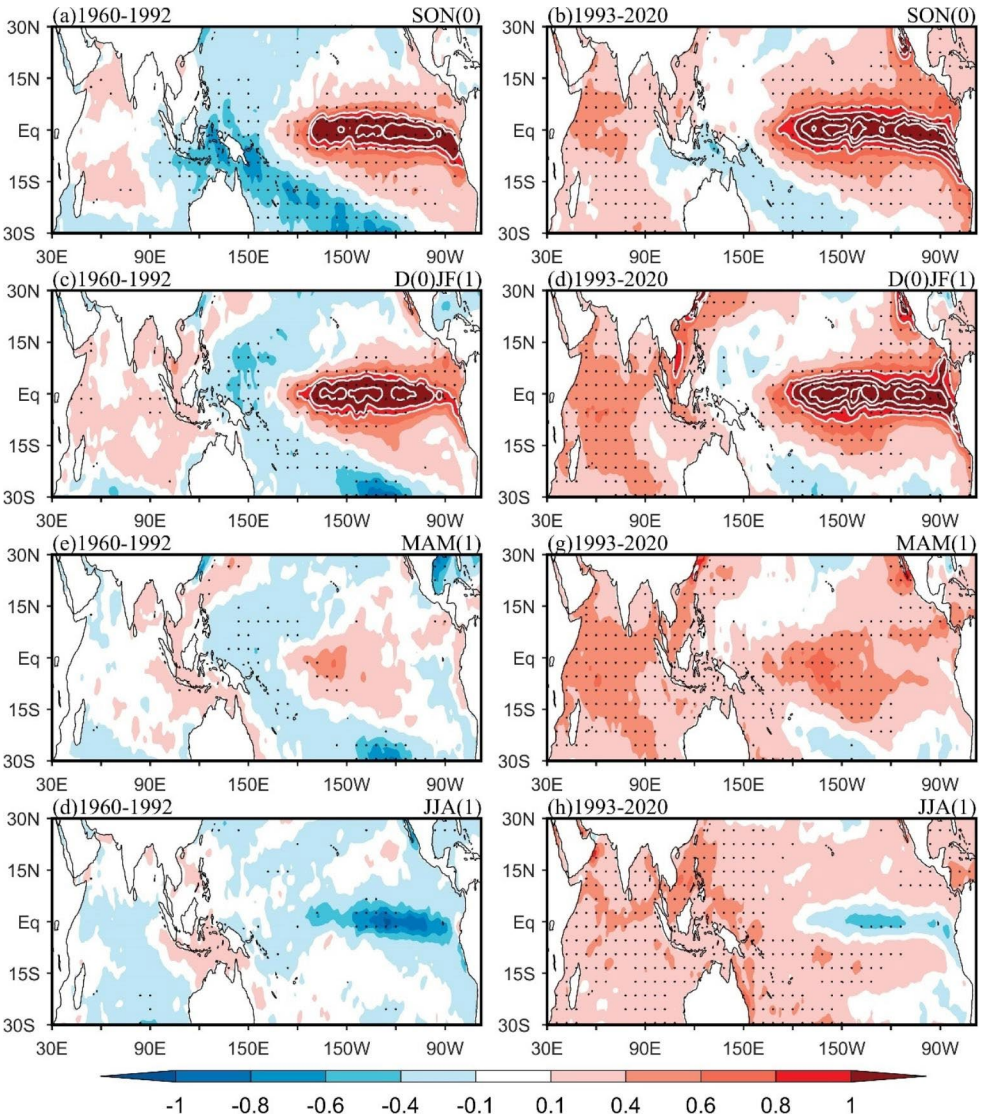

Fig. 5 Composite anomalies of **a** the developing SON, **c** the mature DJF, **e** the decaying spring [March-April-May (MAM)] and **g** the decaying JJA SST (°C) for the El Niño events during 1960–1992. **b**, **d**, **f** and **h** Same as **a**, **c**, **e** and **g**, but for 1993–2020. The white lines denote the SST values larger than 0.8 °C, with the interval of 0.2 °C. The dots in each panel indicate that the composite SST anomalies are at a significance level of $p < 0.05$

surplus precipitation in post-El Niño summers. However, this El Niño-CCSP relationship is unstable, suffering an interdecadal change since the early 1990s. The question is what causes this interdecadal change. We notice that the characters of El Niño also experience an obvious interdecadal change since the early 1990s, featuring an increased intensity as well as a longer duration of the SST anomalies in the tropical central Pacific (Yeh et al. 2009; Lee and McPhaden 2010; McPhaden et al. 2011; Li et al. 2021b). The changed intensity and duration of the El Niño events would certainly cause the change of regional and even global climate responses. Therefore, it might be the reason for the interdecadal change in the relationship between the decaying El Niño and the CCSP.

To demonstrate this, we first examine the interdecadal variation of El Niño. Figure 5 compares the evolutions of the composite SST anomalies for the El Niño events between 1960 and 1992 and 1993–2020. The El Niño events selected in these two epochs are listed in Table 1. From the preceding SON to the following JJA, the SST anomalies in the tropical central and eastern Pacific during these two epochs both exhibit phase-locking characteristics, developing in SON, peaking in DJF and decaying in the following MAM and JJA (Fig. 5). However, the intensity and duration of the El Niño-related SST anomalies between the prior and post epochs are quite different. Compared with the prior epoch, the isotherms larger than 0.8 °C for the El Niño events during the SON (0) and the D(0)JF(1) are more dense and cover a larger area in the post epoch (Fig. 5a-d), indicating that the intensity of El Niño strengthens since the early 1990s. In particular, such strengthened warm SST anomalies feature a westward extension in the post epoch (Fig. 5b, d), which still maintain large values in the MAM(1) (Fig. 5 g). All this suggests that the El Niño-related SST anomalies are stronger and longer-lasting since the early 1990s, especially in the equatorial central Pacific.

Figure 6 further displays the composite monthly evolutions of the Niño3 (5°S-5°N, 150°W-90°W) and Niño4 (5°S-5°N, 160°E-150°W) indices for the El Niño events between the previous and post epochs. Both the Niño3 and Niño4 indices from the SON(0) to the MAM(1) are stronger in the post epoch than those in the prior epoch. Especially, in the El Niño decaying spring, the SST anomalies in the Niño3 and Niño4 regions are both insignificant in the prior epoch. By contrast, in the post epoch, the duration of the significant SST anomalies is longer (Fig. 6a, b). Indeed, the El Niño events are stronger and longer-lasting in the post epoch. Moreover, the strengthened magnitudes of the El Niño-related SST anomalies are greater in the Niño4 region, with the significant Niño4 index also exhibiting a longer duration than the Niño3 index in the MAM(1) for the period 1993–2020 (Fig. 6a, b), indicating that the strengthened intensity and longer duration of the El Niño-related

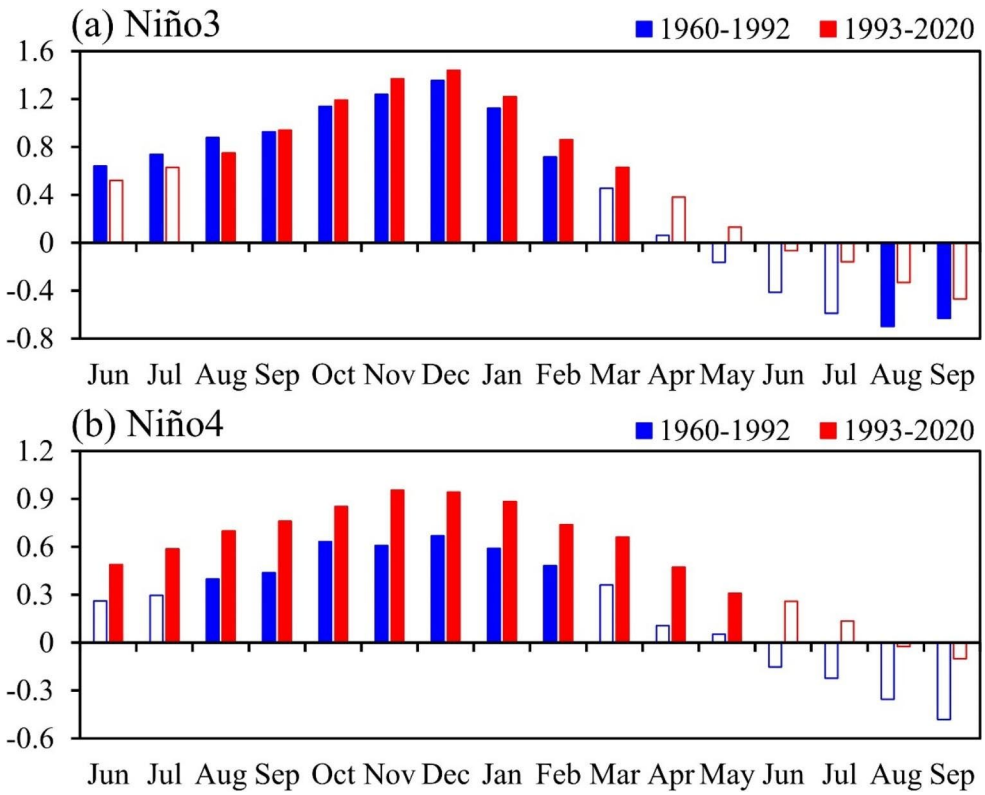

Fig. 6 Composite evolutions of SST anomalies (°C) averaged in **a** the Niño3 region (5°S-5°N, 150°W-90°W) and **b** the Niño4 region (5°S-5°N, 160°E-150°W) from the El Niño developing June to the decaying September during 1960–1992 and 1993–2020. The solid bars are at a significance level of $p < 0.05$

warm SST anomalies in the post epoch are mainly located in the tropical central Pacific.

In Fig. 7, we present the 21-year moving standard deviations (SDs) of the preceding DJF Niño4 index accompanied by the 21-year moving correlations between the preceding DJF Niño3.4 index and the CCSP index. Results show that the variation of the 21-year moving El Niño-CCSP correlations is consistent with the 21-year moving SDs of the Niño4 index, with the correlation coefficient of 0.75, exceeding the significance level of $p < 0.001$. After removing the long-term trend of the 21-year moving SDs and correlations, their correlation coefficient is 0.58 and still at the significance level of $p < 0.001$. This indicates that the changed relationship between the decaying El Niño and the CCSP is closely associated with the changed intensity of the central Pacific warm SST anomalies on both interannual and interdecadal time scales. Since the early 1990s, due to the changed intensity and duration of the El Niño-related warm sea surface temperature (SST) anomalies in the tropical central Pacific, there El Niño-CCSP relationship also experiences an interdecadal change.

4.2 Interdecadal change in the El Niño-induced Indian Ocean responses

In Sect. 4.1, we have identified that there is a strengthened intensity and longer duration of the central Pacific SST anomalies since the early 1990s, which is closely consistent with the changed relationship between the decaying El Niño and the CCSP anomalies. But now it is still unclear how the changed character of El Niño causes the changed El Niño-CCSP relationship. The Indo-Pacific responses are sensitive to the intensity and decaying features of the El Niño events (Xie et al. 2016; Li et al. 2021b). Through the Walker circulation adjustment, we believe that the strengthened intensity and longer duration of the central Pacific SST anomalies may also cause strengthened and longer-lasting easterly wind anomalies along the equatorial Indian Ocean, thus inducing a warmer SWIO in the MAM(1) and a strengthened Indo-Pacific response in the JJA(1) through a series of air-sea interactions. The strengthened Indo-Pacific responses would influence the moisture budget of the central China, thus affecting the CCSP anomalies. This may be the way of the changed character of El Niño mediating the interdecadal relationship between the decaying El Niño and the CCSP.

To demonstrate this, we first composite the evolutions of the 850 hPa wind anomalies averaged between 5°S and 5°N and the SSH anomalies averaged between 5°S to 15°S for the El Niño events during 1960–1992 and 1993–2017 (Fig. 8). Indeed, in response to the strengthened intensity and longer duration of the SST anomalies in the central Pacific since the early 1990s, the equatorial easterly wind anomalies over the Indian Ocean in the post epoch are stronger in the magnitude and longer in the duration, which persist from the preceding October to the following April (Fig. 8b). While in the prior epoch, the anomalous easterlies near the equator are weaker and only persist into February (Fig. 8a). Previous studies have reported that there exists a negative wind curl over the SEIO associated with the equatorial easterly wind anomalies, which can force the downwelling Rossby waves in the ocean, slowly propagating to the west (Masumoto and Meyers 1998; Yu et al. 2005; Xie et al. 2016). As there are different intensity and duration of the equatorial easterly anomalies before and after the early 1990s, the downwelling Rossby waves responses in the South Indian Ocean are also different during these two epochs. Compared with the prior epoch, the downwelling Rossby waves denoted by the SSH

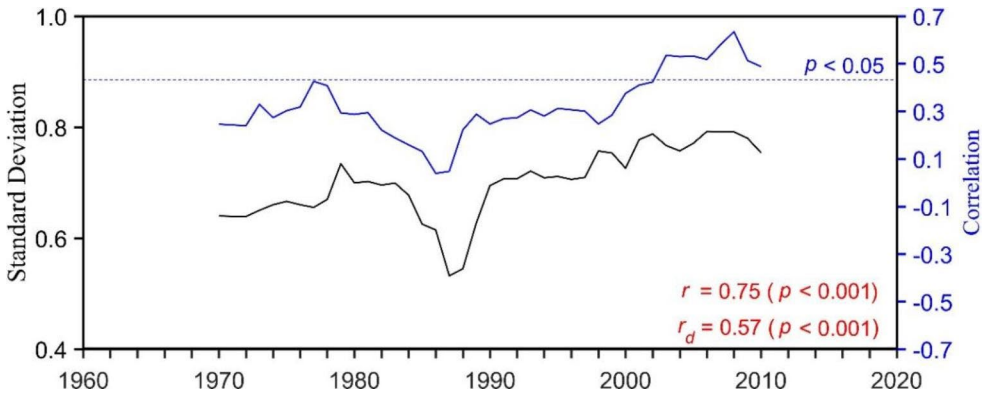

Fig. 7 The 21-year moving standard deviations (SDs) of the DJF Niño4 index (black line) during 1960–2014. The solid blue line is the 21-year moving correlation between the CCSP index and the preceding DJF Niño3.4 index during 1960–2020. r denotes the correlation coefficient between the SDs of the DJF Niño4 index and the 21-year moving correlation of the CCSP index with the preceding DJF Niño3.4 index. r_d is the correlation coefficient between them after removing the long-term trend. The dashed blue line denotes the significance level of $p < 0.05$. All data are linearly detrended and standardized

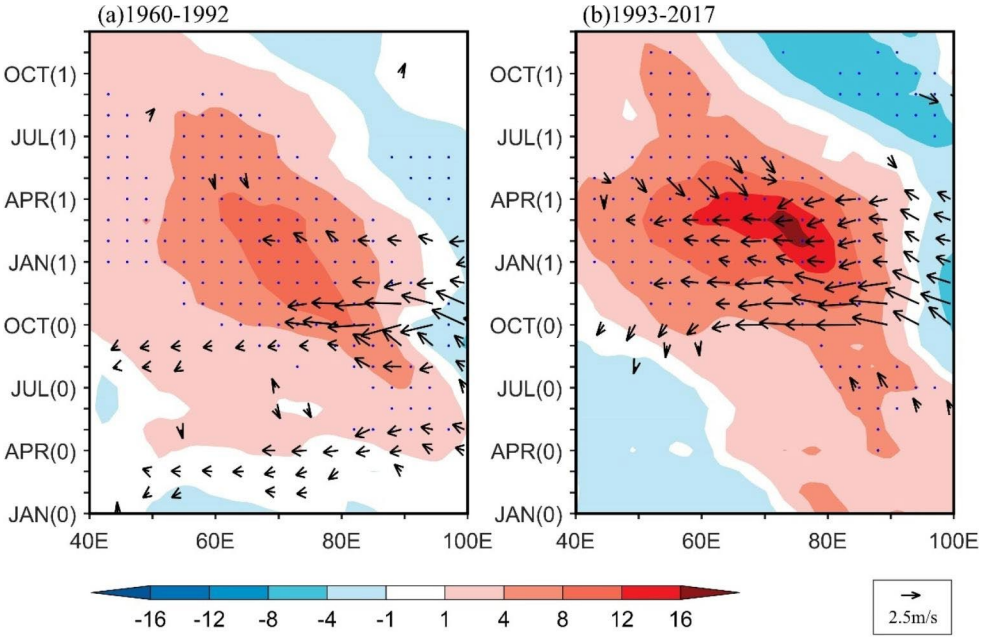

Fig. 8 Time-longitude section of the composite sea surface height anomalies (shaded; cm) averaged from 5°S to 15°S and 850 hPa wind anomalies (arrows; m s^{-1}) averaged from 5°S to 5°N for the El Niño events during **a** 1960–1992 and **b** 1993–2017. The dots in each panel indicate that the sea surface height anomalies are at a significance level of $p < 0.05$. The shown arrows are presented with the zonal or meridional component of the wind anomalies exceeding the confidence level of $p < 0.1$. Wind speeds less than 0.75 m s^{-1} are not shown

anomalies are stronger and longer-lasting in the post epoch. These robust downwelling Rossby waves travel slowly to the west, maximizing in the late-winter and mid-spring. Until April, with the dissipation of the equatorial easterly

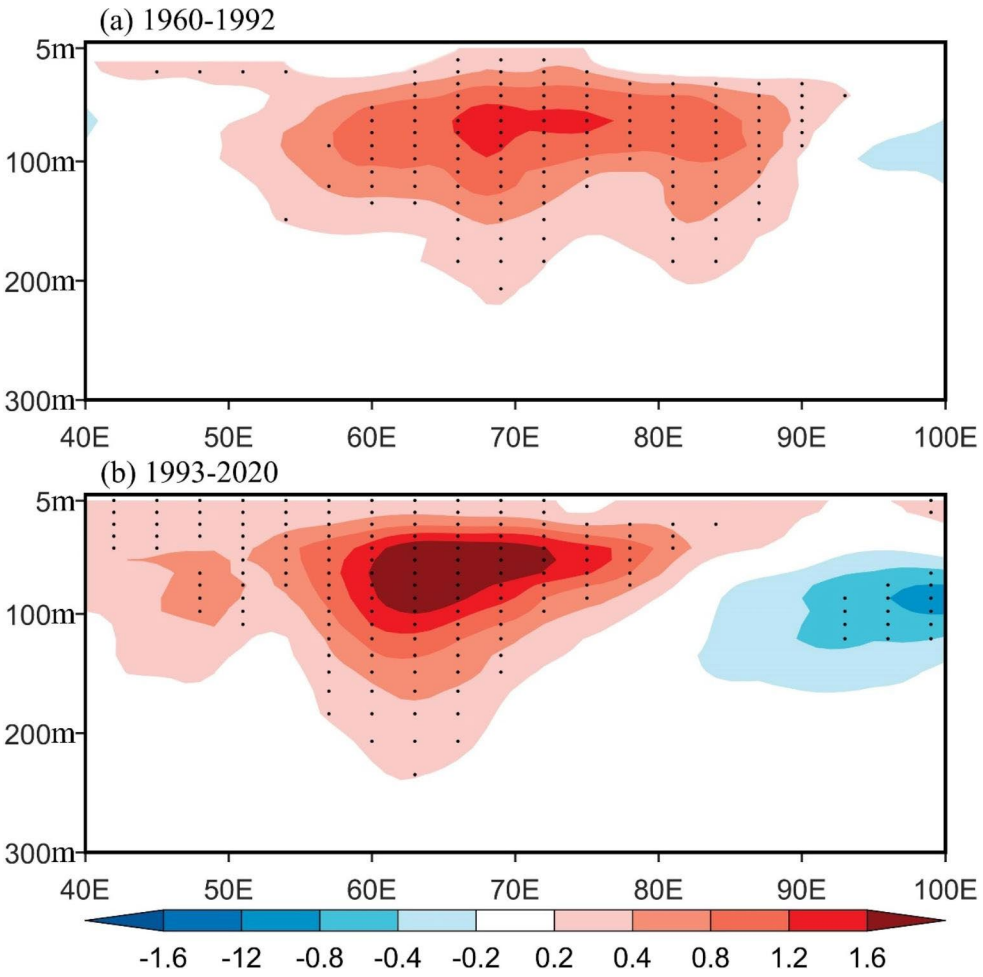

Fig. 9 Depth-longitude profile of the composite spring subsurface ocean temperature anomalies (shaded; °C) averaged from 5°S to 15°S for the El Niño events during **a** 1960–1992 and **b** 1993–2020. The dots in each panel indicate that the subsurface ocean temperature anomalies are at a significance level of $p < 0.05$

anomalies, the SSH anomalies become weaker (Fig. 8b). By contrast, in the prior epoch, such Rossby waves are quite weak, with the peak of the SSH anomalies only half of that in the post epoch (Fig. 8a).

The different Rossby wave responses between the prior and post epochs would cause different thermal conditions in the SWIO via the thermocline feedback. Specifically, the SWIO is special, where the thermocline feedback is active there (Du et al. 2009; Chen et al. 2019). The cyclonic wind curl between the equatorial westerlies and southeasterly trades in the SWIO induces a pronounced open-ocean upwelling and is combined with a shallow thermocline depth all through a year, causing a local minimum in climatological SST (Xie et al. 2016). Such a SWIO thermocline dome is of great importance for the regional climate (Du et al. 2009). As the downwelling Rossby waves propagate into the SWIO thermocline dome, the thermocline would deepen there and therefore result in a pronounced local subsurface to surface warming (Xie et al. 2002; Yukoi et al. 2008; Du et al. 2009). In Fig. 9, we composite the MAM(1) vertical structure of the subsurface ocean temperature anomalies averaged from 5°S to 15°S for the El Niño events during 1960–1992 and 1993–2020. Evidently, in response to enhanced and maintained Rossby waves in the post epoch, more significant warming appears in the subsurface of SWIO in the MAM(1). Such a significant subsurface warming in the SWIO further develops to the surface. As a result, there is a significant SST warming in the SWIO (Fig. 5 g and 9b). By contrast, in the prior epoch, the SWIO subsurface warming is weaker and fails to cause significant warming in the surface (Figs. 5c and 9a).

Such different surface thermal conditions in the SWIO between the prior and post epochs would further cause different atmospheric circulation responses (Wu et al. 2008; Du et al. 2009; Wu and Yeh 2010; Cai et al. 2019; Chen et al. 2019; Chowdary et al. 2019). In Fig. 10, we composite the MAM(1) SST anomalies and 850 hPa wind anomalies for the El Niño events during 1960–1992 and 1993–2020. Clearly, in response to the stronger SWIO SST warming in 1993–2020, there are stronger wind anomalies in the low-level, which feature a C-shaped antisymmetric pattern, with the northeasterlies north and northwesterlies south of the equator (Fig. 10b). By contrast, in the prior epoch, the SST warming in the SWIO as well as the low-level wind

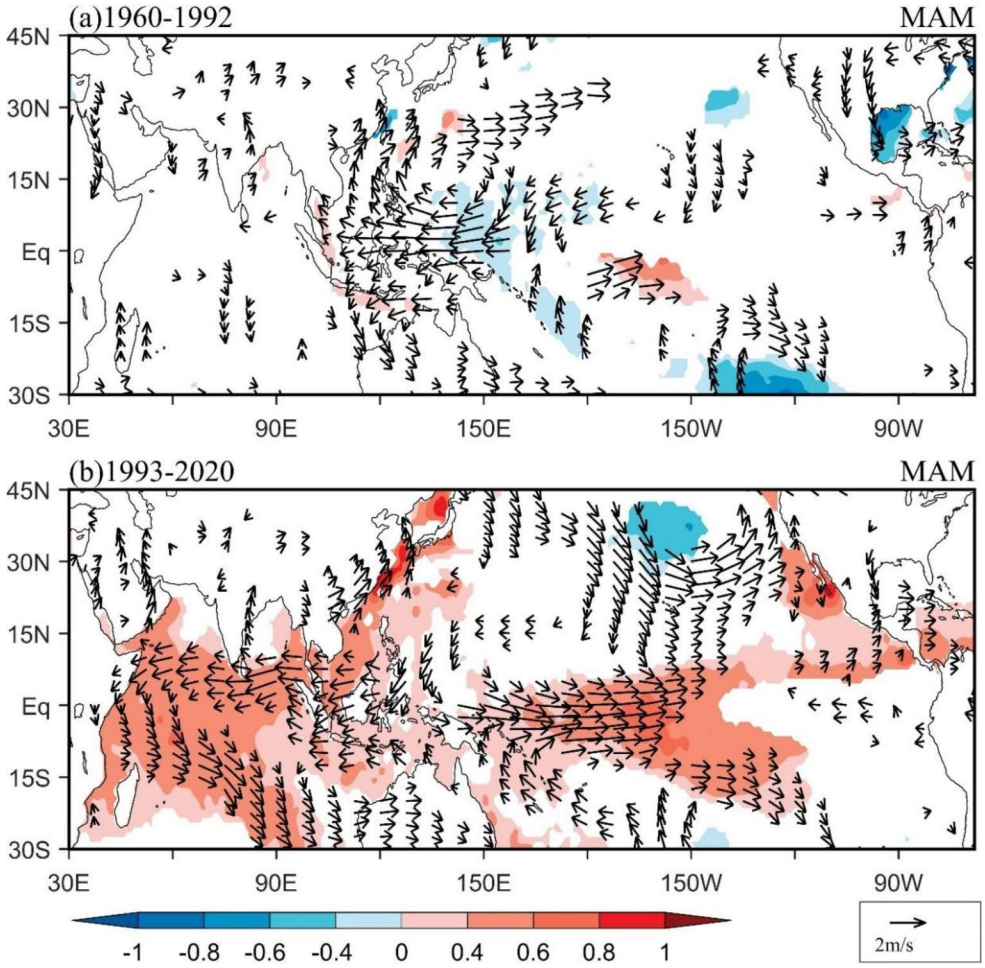

Fig. 10 Composite anomalies of the decaying MAM SST (shaded; °C) and 850 hPa wind (arrows; m s^{-1}) for the El Niño events during **a**1960–1992, **b**1993–2020. The SST anomalies are presented at a significance level of $p < 0.05$. The shown arrows are presented with the zonal or meridional component of the wind anomalies exceeding the significance level of $p < 0.1$. Wind speeds less than 0.5 m s^{-1} are not shown

anomalies over the Indian Ocean are weak and insignificant in the MAM(1) (Fig. 10a).

The different low-level wind anomalies over the SWIO during the El Niño decaying spring between the prior and post epochs could further cause different Indian Ocean SST responses in the JJA(1). This is presented by the composite evolutions of the SST anomalies and 850 hPa wind anomalies averaged between 40°E and 100°E for the El Niño events during 1960–1992 and 1993–2020 (Fig. 11). In the post epoch, the wind anomalies are strong, with a cross-equatorial antisymmetric wind pattern developing in March and persisting into June. This C-shaped wind pattern features a northward migration, with the anomalous northeasterlies occupying the entire NIO in the JJA(1). As a result, such northeasterly wind anomalies can weaken the prevailing southwest monsoon, thus inducing a significant SST warming in the Indian Ocean (Fig. 11b). However, in the prior epoch, the zonal mean wind anomalies are not pronounced throughout the El Niño decaying stage, thus inducing no significant Indian Ocean SST warming in the JJA(1) (Fig. 11a).

4.3 Interdecadal change in the NWPAC and CCSP responses

Figure 12 presents the composite JJA(1) SST anomalies and 850 hPa wind anomalies for the El Niño events during 1960–1992 and 1993–2020. Results further show that there is a warmer Indian Ocean SST in the post epoch. According to the previous studies, the prominent Indian Ocean warming can warm up the troposphere, thus emanating a Kelvin wave penetrating into the Pacific. This equatorial Kelvin wave can induce northeasterly surface wind anomalies in the NWP, thus supporting an anomalous anticyclone there (Xie et al.2009, 2016). Remarkably, in the post epoch, in response to the robust Indian Ocean SST warming, evident anticyclonic anomaly appears in the NWP (Fig. 12b). Such an anomalous anticyclone features a westward extending in its south flank. This would weaken the monsoon westerlies, thus further warming the Indian Ocean. Undoubtedly, the warmer Indian Ocean would, in turn, favor the anomalous NWPAC through the Kelvin waves. Therefore, there is a positive feedback between the NWPAC and the Indian Ocean SST warming in the post epoch. By contrast, in the prior epoch, the anomalous anticyclone is weak, with the

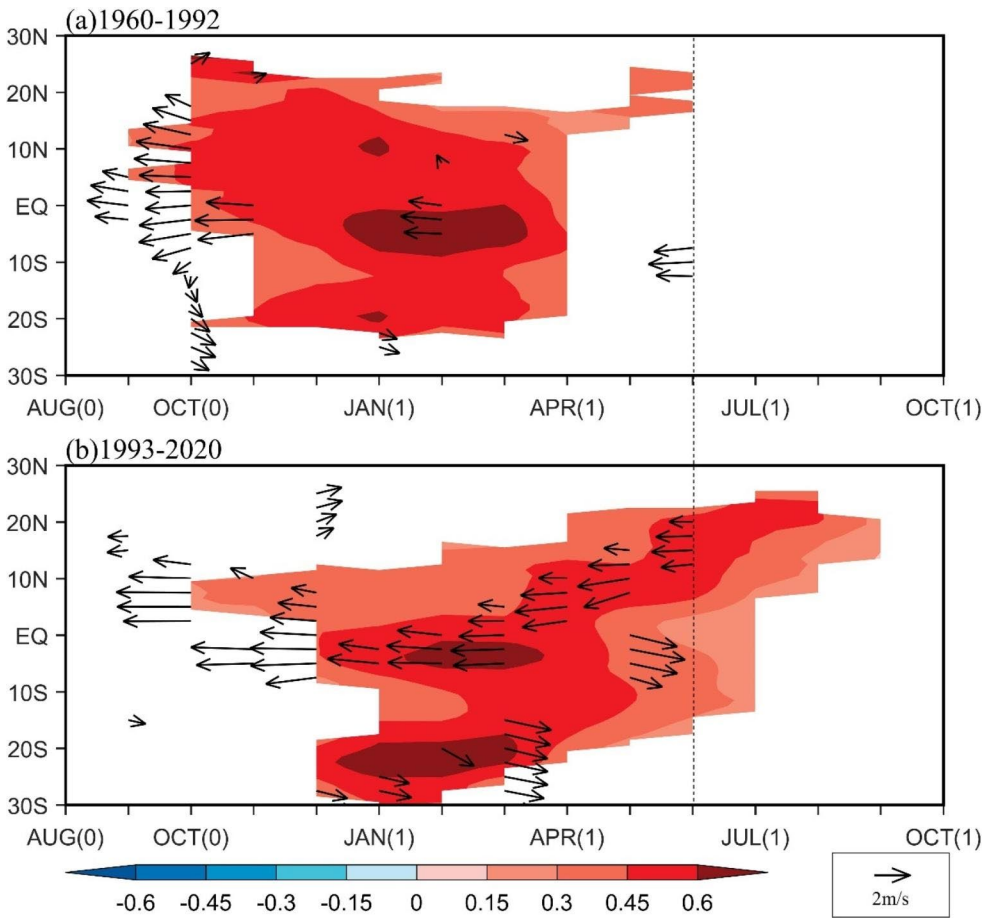

Fig. 11 Time-latitude section of the composite SST anomalies (shaded; °C) and 850 hPa wind anomalies (arrows; m s^{-1}) averaged from 40°E to 100°E for the El Niño events during **a** 1960–1992 and **b** 1993–2020. The SST anomalies are presented at a significance level of $p < 0.05$. The shown arrows are presented with the zonal or meridional component of the wind anomalies exceeding the significance level of $p < 0.1$. Wind speeds less than 0.3 m s^{-1} are not shown

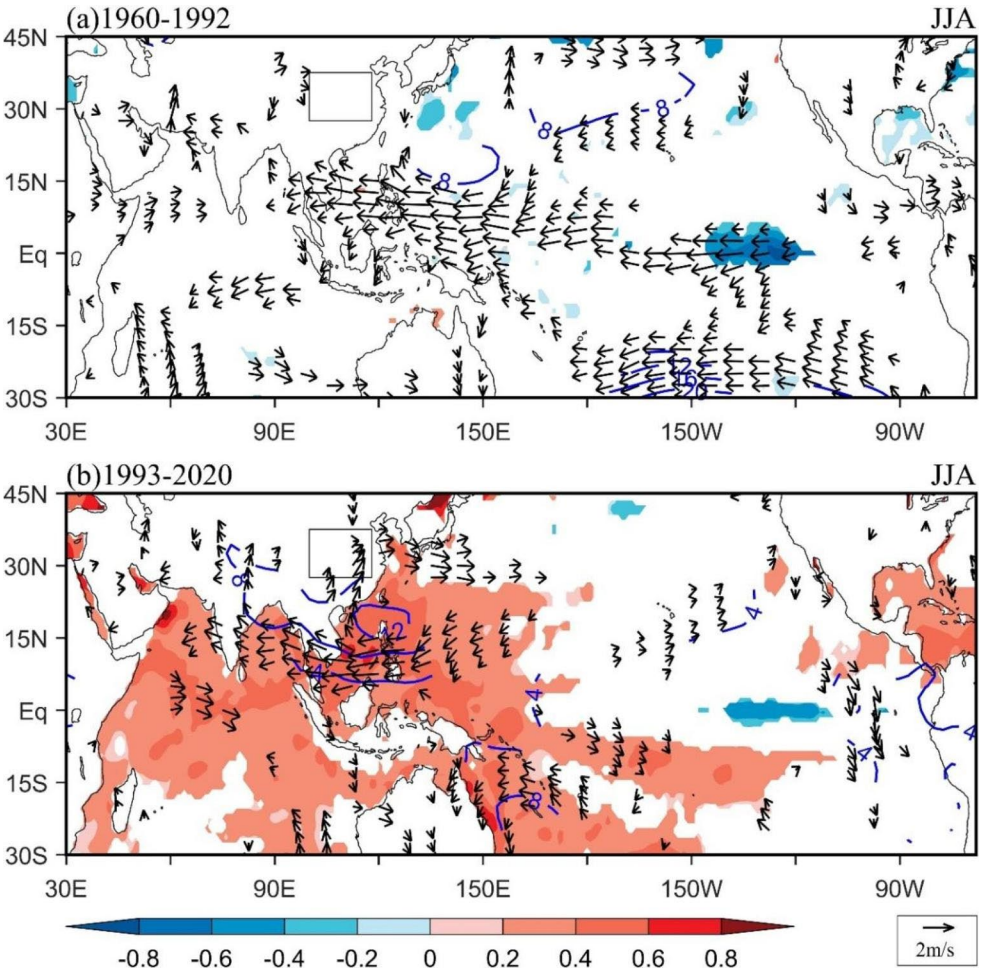

Fig. 12 Composite anomalies of the decaying JJA SST (shaded; °C), 850 hPa wind (arrows; m s^{-1}) and geopotential height (contour; m) for the El Niño events during **a**1960–1992, **b**1993–2020. The SST anomalies and geopotential height anomalies are presented at a significance level of $p < 0.05$. The shown arrows are presented with the zonal or meridional component of the wind anomalies exceeding the significance level of $p < 0.1$. Wind speeds less than 0.5 m s^{-1} are not shown. The box area in each panel denotes the region of the central China

significant part only appearing near the equator (Fig. 12a). Given that there are no evident SST anomalies in the Indian Ocean, the significant part of the anomalous anticyclone may be directly forced by the anomalous cooling

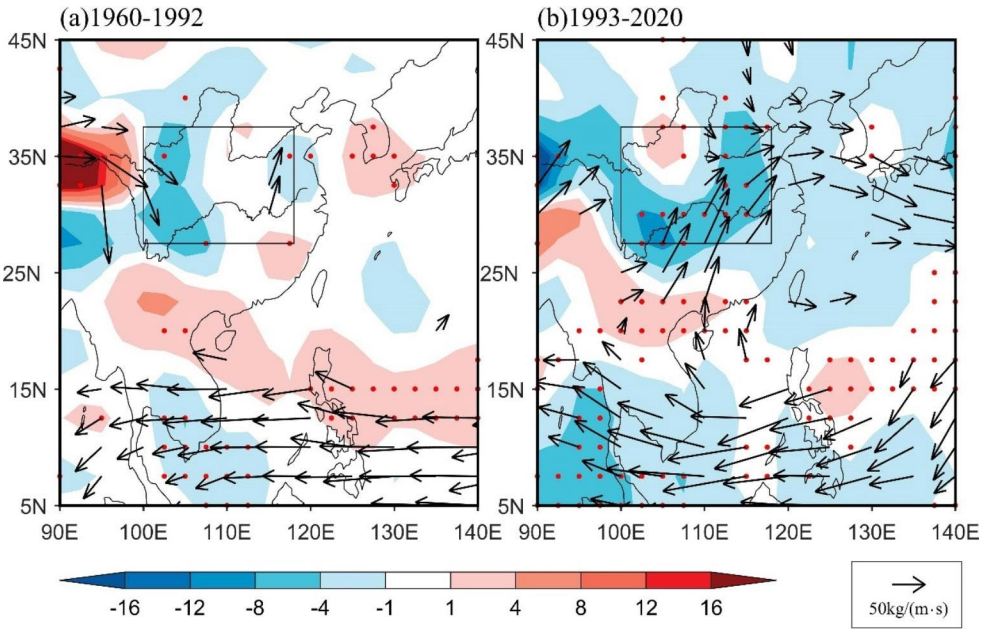

Fig. 13 Composite anomalies of the decaying JJA water vapor flux integrated from 1000 to 300 hPa (arrows; kg m^{-1} s^{-1}) and its divergence (shaded; 10^{-5} kg m^{-2} s^{-1}) for the El Niño events during **a** 1960–1992 and **b** 1993–2020. The dots in each panel indicate that the divergence of the water vapor flux anomalies is at a significance level of $p < 0.1$. The shown arrows are presented with the zonal or meridional component of the water vapor flux anomalies exceeding the significance level of $p < 0.1$. The arrows with water vapor flux anomalies less than 10 kg m^{-1} s^{-1} are not shown. The box area in each panel denotes the region of the central China

in the equatorial central Pacific through the Rossby wave responses (Fig. 12a; Wang et al. 2013, 2017a; Fan et al. 2013; Chen et al. 2016; Li et al. 2017).

The different atmospheric circulation anomalies over the NWP would further cause different moisture budget over the central China. In Fig. 13, the composite JJA(1) water vapor flux anomalies integrated from 1000 to 300 hPa and their divergence for the El Niño events before and after the early 1990s further demonstrate it. Compared with no obvious moisture transporting to the central China in the prior epoch (Fig. 13a), the water vapor transportation is stronger in the post epoch, with the abundant water vapor converging over the central China (Fig. 13b). Note that such water vapor convergence goes especially along the mountainous area of the central China from the southwest to the northeast. This implies that the increased precipitation over the central China may be caused by the orographic uplift under the conditions of the strengthened atmospheric circulations induced by El Niño. All these explain why there are increased precipitation over the central China in the summer when an El Niño event is in its decaying stage since the early 1990s.

Finally, to better understand the interdecadal change in the El Niño-CCSP relationship, we present the relationships among the preceding DJF Niño3.4 index, the following JJA atmospheric circulation anomalies and the CCSP anomalies during the prior and post epochs in Fig. 14. In response to the stronger and longer-lasting SST anomalies in the central Pacific since the early 1990s, the anticyclonic anomalies over the NWP strengthen in the post epoch. When we define the NWPAC index as the zonal wind averaged in the north part of the NWPAC (20°N-35°N, 105°E-120°E) that can deliver the abundant water vapor to the central China, the correlation coefficient between the preceding DJF Niño3.4 index and the following JJA NWPAC index is low and insignificant in the prior epoch (Fig. 14a), while that in the post epoch is 0.52 exceeding the significance level of p

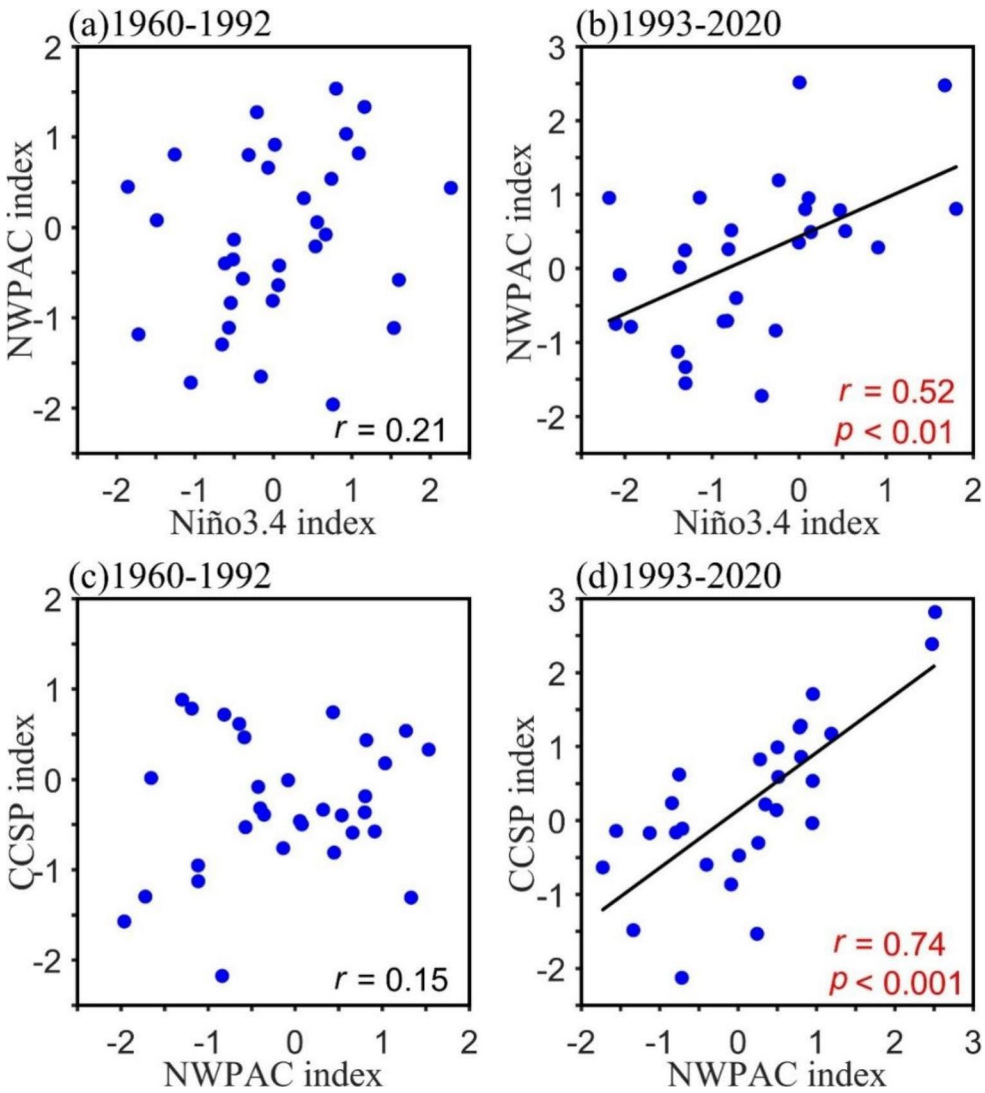

Fig. 14 Scatterplots of **a** the preceding DJF Niño3.4 index and the following JJA Northwest Pacific anticyclone (NWPAC) index, **c** the JJA NWPAC index and the JJA CCSP index during 1960–1992. **b** and **d** Same as **a** and **c**, but for the period 1993–2020

< 0.01 (Fig. 14b). The strengthened NWPAC can enhance the East Asian summer monsoon and transport more water vapor to the central China, thus contributing to increased precipitation there. As a result, the correlation coefficient between the JJA NWPAC index and CCSP index is large and reaches 0.74 ($p < 0.001$) in the post epoch (Fig. 14d). By contrast, the correlation coefficient is not significant in the prior epoch (Fig. 14c).

5 Conclusions and discussions

Summer precipitation over the densely populated central China is of great significance to the local people's livelihood and economic development (Sun et al. 2010; Ren et al. 2013; Ke and Guan 2014; Hu et al. 2020). This study identifies that there is a close relationship between the decaying El Niño and the CCSP. During post-El Niño summers, the central China often suffers surplus precipitation. However, this El Niño-CCSP relationship is unstable, experiencing an interdecadal change since the early 1990s. In the prior epoch (1960–1992), the correlation coefficient between the decaying El Niño and the CCSP is low and insignificant, while that in the post epoch (1993–2020) is dramatically strengthened.

Further analysis suggests that such an interdecadal change between the decaying El Niño and the CCSP is closely associated with the strengthened intensity and longer duration of the El Niño-related SST warming in the central Pacific since the early 1990s. In the post epoch, in response to the stronger and longer-lasting SST warming in the tropical central Pacific, stronger easterly wind anomalies emerge over the equator of the Indian Ocean, which persist from the preceding October to the following April. Such strengthened and longer-lasting equatorial wind anomalies favor an anomalous anticyclone over the SEIO, which constantly forces the downwelling Rossby waves propagating to the west. When the downwelling Rossby waves arrive at the SWIO, where the thermocline is shallow and the thermocline feedback is strong, prominent SST warming appears in this area during the MAM(1). This SWIO SST warming intensifies the atmospheric convection and triggers an antisymmetric wind pattern with the northeasterlies north and the northwestlies south of the equator. In the JJA(1), when the southwest monsoon prevails, the northeasterlies weaken it, thus contributing to a prominent Indian Ocean warming. As a result, significant anticyclonic anomalies appear over the NWP through the Kelvin wave responses induced by the Indian Ocean warming, which enhance the East Asian summer monsoon, bringing more water vapor to the central China and causing increased precipitation there. While in the prior epoch, the intensity as well as the duration of the El Niño-related SST anomalies in the equatorial Pacific is weak, with the Niño4 index in the decaying spring less than half of that in the post epoch. As a result, the equatorial easterly wind anomalies over Indian Ocean weaken and only persist to the following February, inducing less warming in the SWIO in the MAM(1) and thus insignificant Indian Ocean SST warming in the JJA(1). Thus, there are weaker anticyclone over the NWP and thus less precipitation anomalies over the central China.

The present study identifies a strengthened relationship between the decaying El Niño and the following summer precipitation over the central China since the early 1990s and emphasizes the important roles of the preceding autumn and winter intensities as well as the following spring duration of the SST anomalies in the central Pacific for this strengthened relationship. It is reported that such changed character of El Niño originates from a warmer Atlantic due to the positive phase of Atlantic multidecadal oscillation and global warming trend (Yu et al. 2015; Wang et al. 2017b). In a warmer global climate, this implies a higher seasonal prediction skill of the JJA precipitation over the central China if we can comprehensively consider the intensity and duration of El Niño as a prediction factor. Actually, when we combine the intensity (defined as the DJF Niño3.4 index) and duration (defined as $\frac{\text{Niño4(DJF)}-\text{Niño4(MAM)}}{|\text{Niño3.4(DJF)}|}$) of El Niño together, the prediction skill for the CCSP during 1993–2020 is 0.62, which is higher than that using the Niño3.4 index only. Due to the high dependence of the central China on summer precipitation, the improvement of the seasonal prediction of the CCSP is of great potential benefits for the local livelihood of millions of people.

Even though there is an improvement of the El Niño prediction, accurate prediction of the CCSP is still a big challenge. Due to the special location and topography of the central China, the summer climate over the central China is influenced not only by the factors from the tropics but also that from the mid-high latitudes (Ren et al. 2010). Especially, the spring North Atlantic Oscillation (NAO) can result in a triple SST pattern in the North Atlantic, featuring positive (negative) SST anomalies in Northwest Atlantic and negative (positive) SST anomalies in the subpolar and tropical ocean, which can persist through the following summer and exert prominent impact on the East Asian summer climate (Wu et al. 2012; Zuo et al. 2012, 2013; Yim et al. 2014). But it is still unclear to what extent or in what way does the NAO affect the CCSP. A better understanding of these issues will be helpful for the improvement of the seasonal prediction of the CCSP.

Acknowledgements This work was supported by the Natural Science Foundation of China (41831175) and the Fundamental Research Funds for the Central Universities (B210201015).

References

Alexander MA, Bladé I, Newman M et al (2002) The atmospheric bridge: The influence of ENSO teleconnections on air-sea interaction over the global oceans. J Clim 15:2205–2231

Balmaseda MA, Mogensen K, Weaver AT (2012) Evolution of the ECMWF ocean reanalysis system ORAS4. Q J R Meteorol Soc 139:1132–1161

Cai W, Wu L, Lengaigne M, Lengaigne M et al (2019) Pantropical climate interactions. Science 363:1–11

Chang CP, Zhang Y, Li T (2000a) Interannual and interdecadal variations of the East Asian summer monsoon and tropical Pacific SSTs. Part I: Role of the subtropical ridge. J Clim 13:4310–4325

Chang CP, Zhang Y, Li T (2000b) Interannual and interdecadal variations of the East Asian summer monsoon and tropical Pacific SSTs. Part II: Meridional structure of the monsoon. J Clim 13:4326–4340

Chen W (2002) Impacts of El Niño and La Niña on the cycle of the East Asian winter and summer monsoon (in Chinese). Chin J Atmos Sci 26:595–610

Chen ZS, Wen ZP, Wu RG et al (2016) Relative importance of tropical SST anomalies in maintaining the western North Pacific anomalous anticyclone during El Niño to La Niña transition years. Clim Dyn 46:1027–1041

Chen ZS, Du Y, Wen ZP et al (2019) Evolution of south tropical Indian Ocean warming and the climatic impacts following strong El Niño events. J Clim 32:7329–7347

Chen L, Li G, Long SM et al (2021) Interdecadal change in the influence of El Niño in the developing stage on the central China summer precipitation. Clim Dyn (in press). https://doi.org/10.1007/s00382-021-06036-9

Chowdary JS, Gnanaseelan C (2007) Basin-wide warming of the Indian Ocean during El Niño and Indian Ocean dipole years. Int J Climatol 27:1421–1438

Chowdary JS, Xie SP, Lee JY et al (2010) Predictability of summer Northwest Pacific climate in 11 coupled model hindcasts: Local and remote forcing. J Geophys Res Atmos 115:1–16

Chowdary JS, Patekar D, Srinivas G et al (2019) Impact of the Indo-western Pacific Ocean capacitor mode on South Asian summer monsoon rainfall. Clim Dyn 53:2327–2338

Ding Y, Liu Y, Hu ZZ (2021) The record-breaking Meiyu in 2020 and associated atmospheric circulation and tropical SST anomalies. Adv Atmos Sci 6:1–14

Du Y, Xie SP, Huang G, Hu KM (2009) Role of air-sea interaction in the long persistence of El Niño-induced North Indian Ocean warming. J Clim 22:2023–2038

Fan L, Shin SI, Liu QY, Liu ZY (2013) Relative importance of tropical SST anomalies in forcing East Asian summer monsoon circulation. Geophys Res Lett 40:2471–2477

Gao CJ, Li G, Xu B, Li XY (2020a) Effect of spring soil moisture over the Indo-China Peninsula on the following summer extreme precipitation events over the Yangtze River basin. Clim Dyn 54:3845–3861

Gao CJ, Li G, Chen HS, Yan H (2020b) Interdecadal change in the effect of spring soil moisture over the Indo-China Peninsula on the following summer precipitation over the Yangtze river basin. J Clim 33:7063–7082

Harris I, Jones PD, Osborn TJ, Lister DH (2014) Updated high-resolution grids of monthly climatic observations-the CRU TS3.10 dataset. Int J Climatol 34:623–642

He C, Zhou T, Li T (2019) Weakened anomalous western North Pacific anticyclone during an El Niño-decaying summer under a warmer climate: Dominant role of the weakened impact of the tropical Indian Ocean on the atmosphere. J Clim 32:213–230

Hu K, Xie SP, Huang G (2017) Orographically anchored El Niño effect on summer rainfall in central China. J Clim 30:10037–10045

Hu K, Huang G, Xie SP, Long SM (2019) Effect of the mean flow on the anomalous anticyclone over the Indo-Northwest Pacific in post-El Niño summers. Clim Dyn 53:5725–5741

Hu K, Liu Y, Huang G et al (2020) Contributions to the interannual summer rainfall variability in the mountainous area of central China and their decadal changes. Adv Atmos Sci 37:259–268

Jiang WP, Huang G, Huang P et al (2019) Northwest Pacific anticyclonic anomalies during post-El Niño summers determined by the pace of El Niño decay. J Clim 32:3487–3503

Jiang XW, Yang S, Li JP et al (2013) Variability of the Indian Ocean SST and its possible impact on summer western North Pacific anticyclone in the NCEP Climate Forecast System. Clim Dyn 41:2199–2212

Jin DC, Hameed SN, Huo L (2016) Recent changes in ENSO teleconnection over the western Pacific impacts the eastern China precipitation dipole. J Clim 29:7587–7598

Kalnay E, Kanamitsu M, Kistler R et al (1996) The NCEP/NCAR 40-Year Reanalysis Project. Bull Am Meteorol Soc 77:437–471

Ke D, Guan ZY (2014) Regional mean daily precipitation extremes over central China during boreal summer and its relation with the anomalous circulation patterns (in Chinese). Acta Meteorologica Sinica 72:478–493

Kosaka Y, Xie SP, Lau NC, Vecchi GA (2013) Origin of seasonal predictability for summer climate over the northwestern Pacific. Proc Natl Acad Sci USA 110:7574–7579

Lau NC, Nath MJ (2003) Atmosphere-ocean variations in the Indo-Pacific sector during ENSO episodes. J Clim 16:3–20

Lee T, McPhaden MJ (2010) Increasing intensity of El Niño in the central-equatorial Pacific. Geophys Res Lett 37:L14603. https://doi.org/10.1029/2010GL044007

Li G, Jian YT, Yang S et al (2019) Effect of excessive equatorial Pacific cold tongue bias on the El Niño-Northwest Pacific summer monsoon relationship in CMIP5 multi-model ensemble. Clim Dyn 52:6195–6212

Li G, Gao CJ, Lu B, Chen HS (2021a) Inter-annual variability of spring precipitation over the Indo-China Peninsula and its asymmetric relationship with El Niño-South Oscillation. Clim Dyn 56:2651–2665

Li G, Gao CJ, Xu B et al (2021b) Strengthening influence of El Niño on the following spring precipitation over the Indochina Peninsula. J Clim 34:5971–5984

Li T, Wang B, Wu B et al (2017) Theories on formation of an anomalous anticyclone in western North Pacific during El Niño: A review. J Meteorol Res 31:987–1006

Liu BQ, Yan YH, Zhu CW et al (2020) Record-breaking Meiyu rainfall around the Yangtze River in 2020 regulated by the subseasonal phase transition of the North Atlantic Oscillation. Geophys Res Lett 47:e2020GL090342. https://doi.org/10.1029/2020GL090342

Masumoto Y, Meyers G (1998) Forced Rossby waves in the southern tropical Indian Ocean. J Geophys Res 103:27589–27602

McPhaden MJ, Lee T, McClurg D (2011) El Niño and its relationship to changing background conditions in the tropical Pacific Ocean. Geophys Res Lett 38:L15709. https://doi.org/10.1029/2011GL048275

Murtugudde R, McCreary JP, Busalacchi AJ (2000) Oceanic processes associated with anomalous events in the Indian Ocean with relevance to 1997–1998. J Geophys Res 105:3295–3306

Qiao S, Chen D, Wang B et al (2021) The longest 2020 Meiyu season over the past 60 years: Subseasonal perspective and its predictions. Geophys Res Lett 48. https://doi.org/10.1029/2021GL093596. e2021GL093596

Rayner NA, Brohan P, Parker DE et al (2006) Improved analysis of changes and uncertainties in sea surface temperature measured

in situ since the mid-nineteenth century: The HadSST2 dataset. J Clim 19:446–469
Ren GY, Wu H, Chen ZH (2013) Spatial patterns of change trend in rainfall of China (in Chinese). Q J Appl Meteorol 11:322–330
Saji NH, Goswami BN, Vinayachandran PN, Yamagata T (1999) A dipole mode in the tropical Indian Ocean. Nature 401:360–363
Shinoda T, Alexander MA, Hendon HH (2004) Remote response of the Indian Ocean to interannual SST variations in the tropical Pacific. J Clim 17:362–372
Sun J, Xu Y, Chen ZH, Wang K (2010) Characteristics of precipitation in central region of China over 45 years (in Chinese). Resour Environ Yangtze Basin 19:45–51
Sun LY, Yang XQ, Tao LF et al (2021) Changing impact of ENSO events on the following summer rainfall in eastern China since the 1950s. J Clim 34:8105–8123
Takaya Y, Kosaka Y, Watanabe M, Maeda S (2021) Skillful predictions of the Asian summer monsoon one year ahead. Nat Commun 12:2094. https://doi.org/10.1038/s4146-021-22299-6
Tang HS, Hu KM, Huang G et al (2021) Intensification and northward extension of Northwest Pacific anomalous anticyclone in El Niño decaying mid-summer: An energetic perspective. Clim Dyn, in press. https://doi.org/10.1007/s00382-021-05923-5
Tao W, Huang G, Wu RG et al (2017) Asymmetry in summertime atmospheric circulation anomalies over the Northwest Pacific during decaying phase of El Niño and La Niña. Clim Dyn 49:2007–2023
Tao W, Huang G, Wu RG et al (2018) Origins of biases in CMIP5 models simulating Northwest Pacific summertime atmospheric circulation anomalies during the decaying phase of ENSO. J Clim 31:5707–5729
Wang B, Wu RG, Fu XH (2000) Pacific-East Asian teleconnection: How does ENSO affect East Asian. climate? J Clim 13:1517–1536
Wang B, Xiang BQ, Lee JY (2013) Subtropical high predictability establishes a promising way for monsoon and tropical storm predictions. Proc Natl Acad Sci USA 110:2718–2722
Wang B, Li J, He Q (2017a) Variable and robust East Asian monsoon rainfall response to El Niño over the past 60 years (1957–2016). Adv Atmos Sci 34:1235–1248
Wang CZ (2019) Three-ocean interactions and climate variability: A review and perspective. Clim Dyn 53:5119–5136
Wang L, Yu JY, Paek H (2017b) Enhanced biennial variability in the Pacific due to Atlantic capacitor effect. Nat Commun 8:1–7
Wang XD, Xie SP, Guan ZY (2020) Atmospheric internal variability in the summer Indo-northwestern Pacific: Role of the intraseasonal oscillation. J Clim 33:3395–3410
Wang XD, Guan ZY, Jin DC, Zhu J (2021) East Asian summer monsoon rainfall anomalies in 2020 and the role of Northwest Pacific anticyclone on the intraseasonal-to-interannual timescales. J Geophys Res Atmos 126:e2021JD34607. https://doi.org/10.1029/2021JD034607
Wu B, Zhou TJ, Li T (2009) Seasonally evolution dominant interannual variability modes of East Asian climate. J Clim 22:2992–3005
Wu B, Li T, Zhou T (2010) Relative contributions of the Indian Ocean and local SST anomalies to the maintenance of the western North Pacific anomalous anticyclone during the El Niño decaying summer. J Clim 23:2974–2986
Wu RG, Kirtman BP, Krishnamurthy V (2008) An asymmetric mode of tropical Indian Ocean rainfall variability in boreal spring. J Geophys Res Atmos 113:D05104. https://doi.org/10.1029/2007JD009316
Wu RG, Yeh SW (2010) A further study of the tropical Indian Ocean asymmetric mode in boreal spring. J Geophys Res Atmos 115:D08101. https://doi.org/10.1029/2009JD012999
Wu X, Li G, Jiang W et al (2021) Asymmetric relationship between ENSO and the tropical Indian Ocean summer SST anomalies. J Clim 34:5955–5969
Wu Z, Li J, Jiang Z et al (2012) Possible effects of the North Atlantic Oscillation on the strengthening relationship between the East Asian summer monsoon and ENSO. Int J Climatol 32:794–800
Xie SP, Hu K, Hafner J et al (2009) Indian Ocean capacitor effect on Indo-western Pacific climate during the summer following El Niño. J Clim 22:730–747
Xie SP, Kosaka Y, Du Y et al (2016) Indo-western Pacific Ocean capacitor and coherent climate anomalies in post-ENSO summer: A review. Adv Atmos Sci 33:411–432
Yang JL, Liu QY, Xie SP et al (2007) Impact of Indian Ocean SST basin mode on the Asian summer monsoon. Geophys Res Lett 34:L02708. https://doi.org/10.1029/2006GL028571
Yeh SW, Kug JS, Dewitte B et al (2009) El Niño in a changing climate. Nature 461:511–514
Yim SY, Wang B, Kwon MH (2014) Interdecadal change of the controlling mechanisms for East Asian early summer rainfall variation around the mid-1990s. Clim Dyn 42:1325–1333
Yu JY, Kao PK, Paek H et al (2015) Linking emergence of the central Pacific El Niño to the Atlantic Multidecadal Oscillation. J Clim 28:651–662
Yu WD, Xiang BQ, Liu L, Liu N (2005) Understanding the origins of internanual thermocline variations in the tropical Indian Ocean. Geophys Res Lett 32:L24706. https://doi.org/10.1029/2005GL024327
Xie SP, Du Y, Huang G et al (2010) Decadal shifting in El Niño influences on Indo-western Pacific and East Asian climate in the late 1970s. J Clim 23:3352–3368
Zhang R, Sumi A, Kimoto M (1999) A diagnostic study of the impact of El Niño on the precipitation in China. Adv Atmos Sci 16:229–241
Zhang RH, Min QY, Su JZ (2017) Impact of El Niño on atmospheric circulations over East Asia and rainfall in China: Role of the anomalous western North Pacific anticyclone. Sci China Earth Sci 60:1124–1132
Zheng J, Wang C (2021) Influences of three oceans on record-breaking rainfall over the Yangtze River Valley in June 2020. Sci China Earth Sci 64. https://doi.org/10.1007/s11430-020-9758-9
Zhou X, Liu F, Wang B et al (2019) Different responses of East Asian summer rainfall to El Niño decays. Clim Dyn 53:1497–1515
Zhou ZQ, Xie SP, Zhang GJ, Zhou W (2018) Evaluating AMIP skill in simulating interannual variability over the Indo-western Pacific. J Clim 31:2253–2265
Zhou ZQ, Xie SP, Zhang RH (2021) Historic Yangtze flooding of 2020 tied to extreme Indian Ocean conditions. Proc Natl Acad Sci USA 118:2022255118. https://doi.org/10.1073/pnas.2022255118
Zuo J, Li W, Ren H, Chen L (2012) Change of the relationship between the spring NAO and East Asian summer monsoon and its possible mechanism. Chin J Geophys 55:23–34
Zuo J, Li W, Sun C et al (2013) Impact of the North Atlantic sea surface temperature tripole on the East Asian summer monsoon. Adv Atmos Sci 30:1173–1186